


Holocene migration of oceanic front systems over the Conrad Rise in the Indian Sector of the Southern Ocean



KOTA KATSUKI,^{1*} MINORU IKEHARA,² YUSUKE YOKOYAMA,³ MASAKO YAMANE³ and BOO-KEUN KHIM⁴

¹Surficial Environment & Global Change Department, Korea Institute of Geoscience and Mineral Resources, Daejeon 305-350, Korea

²Center for Advanced Marine Core Research, Kochi University, Japan

³Atmosphere and Ocean Research Institute, University of Tokyo, Japan

⁴Department of Oceanography, Pusan National University, Korea

Received 8 October 2010; Revised 4 July 2011; Accepted 6 July 2011

ABSTRACT: There has been limited previous research about Holocene climate variability in the Indian Sector of the Southern Ocean. Here we examine centennial-scale changes in diatom assemblages and stable isotopic ratios since 10 000 cal a BP in a high-accumulation-rate sediment core from the Conrad Rise. Although abundances of dominant diatom taxa (*Fragilariopsis kerguelensis* and *Thalassiothrix antarctica*) are comparatively constant, relative abundances of secondary taxa fluctuate. Before c. 9900 cal a BP, winter sea-ice and cold water covered the Conrad Rise. Following deglaciation the sea-ice retreated from the Conrad Rise, lagging that of the Atlantic and eastern Indian Sectors by about 1500 a. The Polar Front moved southward during the early Holocene optimum and north Antarctic Zone waters covered the Conrad Rise for about 650 a. After 9300 cal a BP, solar insolation strongly influenced sea surface temperature and primary productivity in the Southern Ocean. In the high-latitude Indian Sector, productivity increased 1500 a after the onset of late Holocene neoglaciation. Periodic $\delta^{18}\text{O}$ and cold-water diatom taxa spikes (at intervals of 200 and 300–500 a, respectively) occurred after 9300 cal a BP, probably associated with solar activity. Fluctuations in short-term sea surface temperature and cold-water taxa are synchronous with changes in δD observed in an east Antarctic ice core. Copyright © 2011 John Wiley & Sons, Ltd.

KEYWORDS: Conrad Rise; diatom; Holocene; oceanic front; Southern Ocean.

Introduction

The Polar Frontal Zone (PFZ, defined as an area within 1° latitude of the Antarctic Polar Front, APF) is one of the highest opal sediment accumulation regions in the Southern Ocean (e.g. Bareille *et al.*, 1991). Diatoms preserved in the sediments of the PFZ provide information on the local oceanographic and regional climate system. To date, only a limited number of palaeoenvironmental and micropalaeontological studies have been conducted in the PFZ of the Southern Ocean (e.g. Dezileau *et al.*, 2003; Nielsen *et al.*, 2004).

Here we attempt to reconstruct Holocene sea-surface environmental changes based on quantitative assessment of fossil diatom assemblages and stable isotopes of planktonic foraminifera from a sediment core collected from the Conrad Rise in the Indian Sector of the Southern Ocean. We pay particular attention to the history of sea-ice cover in terms of surface-water properties and the relationship between the Antarctic marine environment and atmosphere–ocean linkages.

Oceanographic setting

The Southern Ocean is divided into the several zones by the wind-induced Antarctic Circumpolar Current (ACC) (Belkin and Gordon, 1996). Each zone is characterized by differences in surface-water temperature and salinity. The zonal boundaries are called fronts, and four major fronts are recognized: from north to south, the Subtropical Front (STF), Subantarctic Front (SAF), APF and Southern ACC Front (SACCF, or Southern Boundary of the ACC: SB) (e.g. Orsi *et al.*, 1995). In the Indian Sector of the Southern Ocean, these fronts have a complex

alignment as a result of the convoluted sea bed topography. Therefore, several fronts have been described south of the APF (for more detail, see Pollard *et al.*, 2002).

The Conrad Rise is located between the APF and SACCF under the ACC, in a region called the Antarctic Zone (AAZ) (Fig. 1). The APF is identified by the northernmost extent of the 2°C subsurface temperature minimum (Belkin and Gordon, 1996; Sparrow *et al.*, 1996). The AAZ is also defined by salinity, which is more important than temperature in controlling the stratification of the upper ocean. The APF is an important climate boundary with respect to heat and salt budgets and primary production in the surface ocean (de Baar *et al.*, 1995; Bathmann *et al.*, 1997). Large biogenic sediment accumulation rates of diatom ooze occur in the area of the PFZ, resulting in reduced opal dissolution and high opal export flux (e.g. Lisitzin, 1972; Zielinski and Gersonde, 1997). The SACCF is located close to the northernmost limit of winter sea-ice. In the south-west Indian Sector of the Southern Ocean, the latitude of the winter sea-ice edge fluctuates annually between 59 and 63°S (e.g. Simmonds and Jacka, 1995).

The ACC branches at the western end of the Conrad Rise to form two intense jets, with speeds reaching 17 cm s⁻¹, that in general flow over regions with a water depth of 3000–3500 m. In contrast, relatively slow-moving water, flowing at 0–5 cm s⁻¹, covers the Conrad Rise itself (Durgadoo *et al.*, 2008).

Dune-like bedforms (mudwaves) exist on the south-west slope of the Conrad Rise. These mudwaves are about 30 m high with a wavelength of a few hundred metres. The bedforms are observed at water depths of 2000–3200 m. Similar wavy sedimentary structures are recognized below the seafloor in seismic profiles of the Conrad Rise (H. Oiowane, Y. Nakamura, M. Ikehara, Y. Suganuma, T. Sato, Y. Nogi and H. Miura, unpubl. data).

*Correspondence: K. Katsuki, as above.
E-mail: kkota@kigam.re.kr

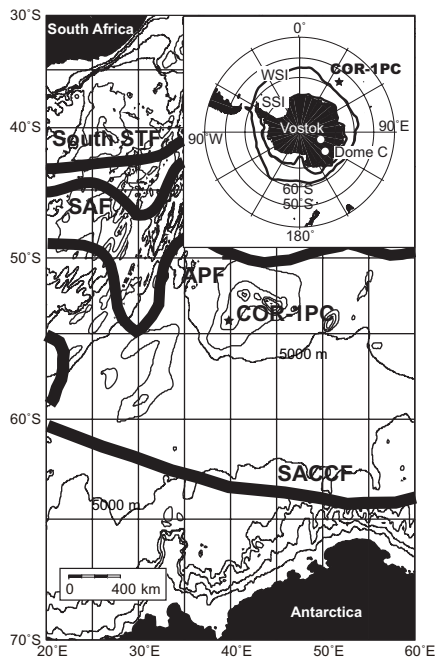


Figure 1. Map showing the bathymetry and zonal front patterns in the Indian Sector of the Southern Ocean. The contour interval is 1000 m. Oceanographic information is from Orsi *et al.* (1995) and Belkin and Gordon (1996). Abbreviations: WSI, winter sea-ice edge; SSI, summer sea-ice edge. Star, sediment core COR-1PC site; circles, ice cores (Vostok and Dome C). Map was drawn by Online Map Creation.

Materials and methods

Piston core COR-1PC (54°16.04'S, 39°46.00'E; water depth, 2864 m; core length, 408 cm) was collected from the southwest flank of the Conrad Rise during Cruise KH07-04 by R/V *Hakuho-Maru* in January 2008 (Fig. 1). The core sediments comprise mainly diatom ooze (Fig. 2). There are no signs of unconformities throughout the sample core. Sediment colour is mainly white, although it is green–brown in the lowermost 10 cm.

Age control for the core is provided by accelerator mass spectrometry (AMS) ^{14}C dating of the planktonic foraminifer *Neogloboquadrina pachyderma* (sinistral) (Table 1). Seven radiocarbon samples were treated according to the protocol described by Yokoyama *et al.* (2007, 2010) with target graphites measured at the AMS facility Micro Analysis Laboratory, Tandem accelerator (MALT), at the University of Tokyo. All dates are corrected for the reservoir age (890 a) of the Southern Ocean (Bard, 1988) and converted to calendar years (cal a BP) using the calibration program CALIB 5.0.2 (Stuiver *et al.*, 1998). Linear sediment accumulation rates calculated between age model points are as high as 34.9–52.4 cm ka $^{-1}$,

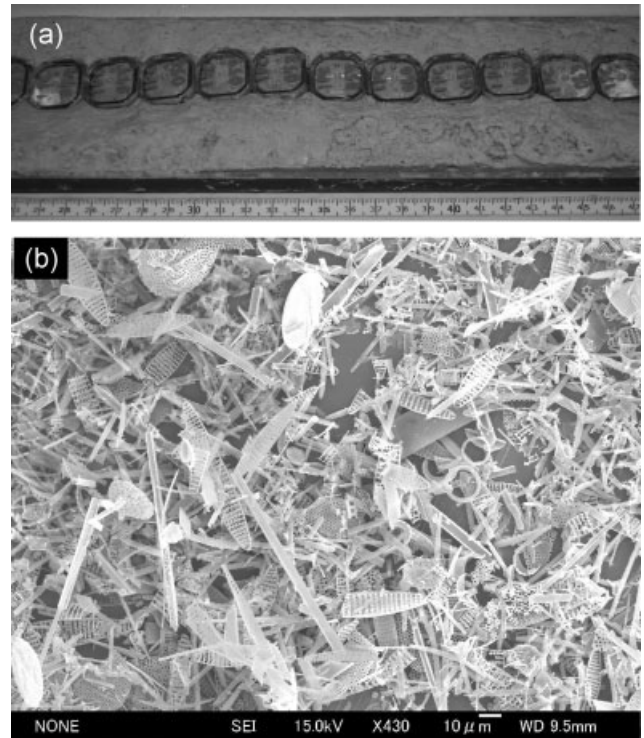


Figure 2. (a) Photograph of split core COR-1PC, 127.6–149.6 cm depth, with a succession of sampling cubes. (b) Scanning electron micrograph of core COR-1PC components at 430 \times magnification, from 27.2 cm depth.

except in the top 50 cm of the core which had a rate of 17.1 cm ka $^{-1}$. The average sedimentation rate for the entire core is 41.5 cm ka $^{-1}$.

We analysed the diatom content of the core sediments in 99 samples. The sampling interval was 2.2 and 4.4 cm (equivalent to about 80 and 160 a, respectively) and sediments were mounted in Pleurax on glass slides for counting. All diatoms were identified and counted until 400 individual valves were counted. Specimens representing more than half of a valve were counted as one specimen; for pennate diatoms, each pole was counted as half a specimen. Counts are expressed as percentages of the total assemblage. Observations were made under a light microscope at 1000 \times magnification.

For foraminifera analysis sediments were washed with water through a 63- μm -mesh sieve, and the residual samples on the sieve were dried at 50°C. Tests of the planktonic foraminifer *N. pachyderma* (sinistral) larger than 180 μm in size were then picked for stable isotope analysis. The sampling interval for $\delta^{18}\text{O}$ analysis was 2.2 cm, corresponding to about 80 a per sample. The tests (50 specimens per sample) were cleaned ultrasonically with methanol, slightly crushed in a glass vial and weighed. Approximately 100 μg of the crushed specimens was

Table 1. Radiocarbon ages of planktonic foraminifera [*Neogloboquadrina pachyderma* (sinistral)] from core COR-1PC.

Sample ID	Top (cm)	Bottom (cm)	Mid-depth (cm)	^{14}C age (a BP)	Calibrated age range (a BP) (1 σ)	Calibrated age (cal a BP)	MTC* code	Sedimentation rate (cm a $^{-1}$)
1–2	17.0	21.6	19.3	1770 \pm 90	732–909	820	12256	
15	48.9	51.2	50.0	1950 \pm 55	935–1060	1000	13311	170.6
37	99.0	101.3	100.2	2825 \pm 80	1858–2057	1960	12092	52.3
82–83	199.8	204.3	202.1	5095 \pm 70	4766–4927	4845	12257	35.3
104–105	249.5	254.0	251.7	6285 \pm 90	6104–6305	6205	12258	36.5
149	350.2	352.5	351.3	8785 \pm 75	8742–8973	8860	12259	37.5
171	400.2	402.5	401.3	9730 \pm 100	9907–10 182	10 045	11550	42.2

*MTC, Micro Analysis Laboratory, Tandem accelerator (MALT), University of Tokyo.

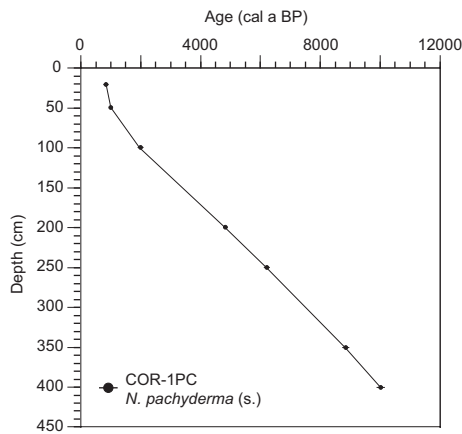


Figure 3. Age–depth relationship of sediments from the Conrad Rise (COR-1PC).

reacted with 100% phosphoric acid at 90°C in a vacuum. The released CO₂ was purified and analysed for $\delta^{18}\text{O}$ using an IsoPrime isotope ratio mass spectrometer with a MultiPrep automated sample preparation module (GV Instruments Ltd) at Kochi University. The results are expressed relative to the VPDB (Vienna PeeDee Belemnite) standard. The estimated analytical precision is better than $\pm 0.05\%$ for both $\delta^{18}\text{O}$ and $\delta^{13}\text{C}$ measurements.

Results

Rapid accumulation of diatomaceous sediment in the form of diatom mats on the Conrad Rise is attributable to *Thalassiothrix*

antarctica, a long, slender diatom that provides a framework to be filled by *Fragilariopsis kerguelensis* (Figs 2b and 3). The relative abundance of *F. kerguelensis* exceeded 65% throughout the core, except at the bottom.

Although the major diatom constituents remained almost the same throughout the core, the relative abundance of minor constituent taxa, including *Eucampia antarctica*, *Fragilariopsis ritscheri*, and *F. curta*, showed a rapid decrease at about 9900 cal a BP. Before 9900 cal a BP these taxa exceeded 5% of the total diatom valves. Another minor taxon, *Thalassionema nitzschioides* var. *lanceolata*, significantly increased in abundance between 9900 and 9300 cal a BP. The remaining minor taxa, including *F. sepranda*, *F. rhombica* and *Thalassiosira gracilis* var. *gracilis*, showed periodic spikes after 9300 cal a BP (Fig. 4).

The $\delta^{13}\text{C}$ and $\delta^{18}\text{O}$ values of *N. pachyderma* (sinistral) shifted abruptly at about 10 200 cal a BP (Fig. 5), after which the $\delta^{13}\text{C}$ values gradually increased until 2600 cal a BP, whereas the $\delta^{18}\text{O}$ values began to decrease after 4000 cal a BP.

Discussion

Rapid environmental changes resulting from the migration of oceanographic fronts during deglaciation

We divide the diatom assemblages in core COR-1PC into three stages: (i) prior to 9900 cal a BP, (ii) 9900–9300 cal a BP and (iii) after 9300 cal a BP. The first stage is characterized by a rapid increase in the abundance of *Fragilariopsis curta*, *F. ritscheri* and *Eucampia antarctica* (Fig. 4). The frequency of *F. curta* provides a proxy for the position of the winter sea-ice

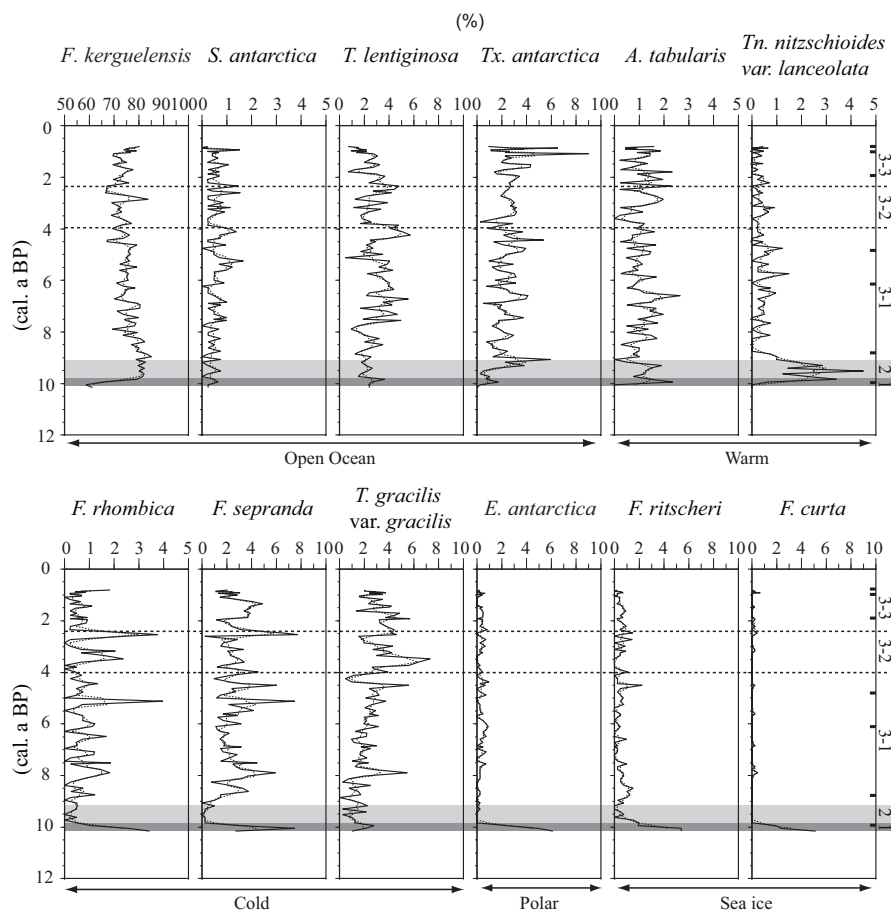


Figure 4. Temporal variation of relative abundance of 12 major diatom species from core COR-1PC. The dashed line represents the three-point running average. The stages discussed in the text are indicated on the right of the figure; dark and light shading indicate stages 1 and 2, respectively. Light shading (stage 2) indicates the EHO. Short bold bars along the right side mark the depths of materials dated by ¹⁴C analysis.

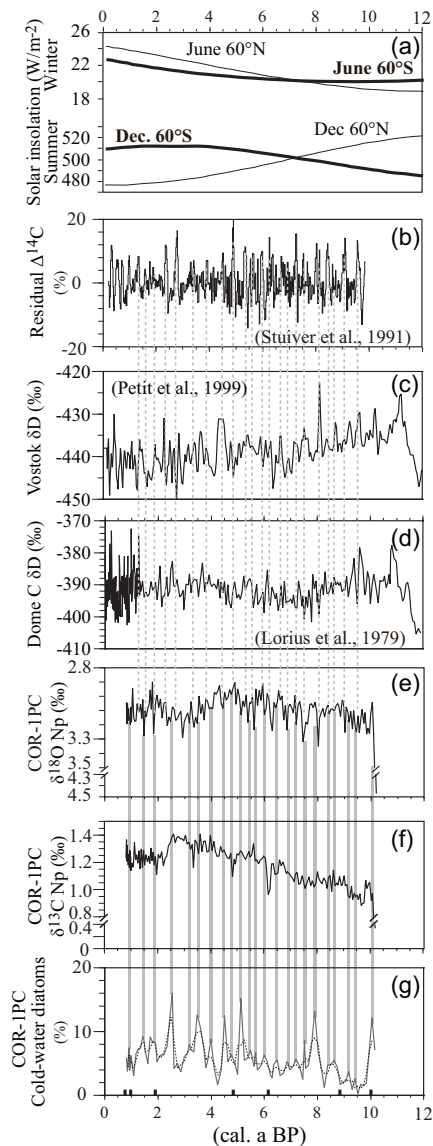


Figure 5. A comparison of (a) solar insolation (summer and winter at 60°N and 60°S) with: (b) residual $\Delta^{14}\text{C}$ after removing the long-term (400-a average) tendency (modified from Stuiver *et al.*, 1991); (c) downcore variations in δD from the Vostok ice core (Petit *et al.*, 1999); (d) downcore variations in δD from the Dome C ice core (Lorius *et al.*, 1979); (e, f) $\delta^{18}\text{O}$ and $\delta^{13}\text{C}$ values from planktonic foraminifera; and (g) total relative abundance of three cold-water diatom taxa (*Fragilariopsis sepranda*, *Fragilariopsis rhombica* and *Thalassiosira gracilis* var. *gracilis*) from core COR-1PC. Shaded bars indicate synchronous peaks between $\delta^{18}\text{O}$ values and cold-water diatom taxa in core COR-1PC, and broken bars in (b)–(e) indicate peaks of residual $\Delta^{14}\text{C}$. Short bold bars at the bottom mark the locations of materials used for ^{14}C analyses.

edge and of waters that are influenced by spring melt-back. An abundance of about 1–3% of this taxon is considered diagnostic of the maximum winter ice-edge (Gersonde and Zielinski, 2000). *F. ritscheri* is observed in the sea-ice region (Armand *et al.*, 2005) and a high percentage (up to 8%) of *E. antarctica* makes a distinct appearance to the north of the present-day winter sea-ice edge (e.g. Zielinski and Gersonde, 1997). The timing of changes in these taxa coincides with clear variations in $\delta^{18}\text{O}$ and $\delta^{13}\text{C}$ values (Figs. 4 and 5).

Our results suggest that the northern winter sea-ice limit covered the Conrad Rise before 9900 cal a BP but this was replaced by cold water after this date (Fig. 6a). A similar trend has been reported in the Atlantic (e.g. Gersonde *et al.*, 2003; Bianchi and Gersonde, 2004) and central Indian Ocean

(Dezileau *et al.*, 2003). However, the sea-ice retreat in these regions was about 1500 a earlier than that recorded at the Conrad Rise. For example, sea-ice retreated from the eastern Atlantic Sector of the Indian Ocean at 53°S at about 12 000 cal a BP (Bianchi and Gersonde, 2004). Changes in δD from east Antarctic ice cores (e.g. Vostok, Dome C, Dome B and Komsomolskaia) show that atmospheric warming occurred at c. 12 000–11 000 cal a BP (e.g. Petit *et al.*, 1999; Masson *et al.*, 2000; Jouzel *et al.*, 2001) (Fig. 5). We therefore infer that the sea-surface environment at the Conrad Rise was controlled by the position of local oceanographic fronts rather than by regional atmospheric warming during the early Holocene. Seasonal sea-ice and cold water masses persisted for about 1500 a longer at the Conrad Rise in comparison with the overall timing of Southern Hemisphere sea-ice retreat and increases in air temperature (e.g. Masson *et al.*, 2000; Stenni *et al.*, 2001; Morgan *et al.*, 2002).

Why were the oceanographic changes at the Conrad Rise delayed compared with other regions? Crosta *et al.* (2007) reported that the timings of climatic periods in the Southern Ocean are not in phase and that this may reflect discrepancies in core stratigraphies and/or real differences in regional climates. We suggest that a lag of 1500 a is too large to be attributed to problems in stratigraphy and resolution. A more likely explanation for this lag is a different evolution of regional climate at this site.

Variations in solar insolation are regarded as one of the primary climatic forcing mechanisms (Paillard, 1998). In core COR-1PC, the summer solar insolation pattern at 60°S (Berger, 1978) is similar to the $\delta^{13}\text{C}$ curve (Fig. 5). This similarity suggests that summer solar insolation is a major climate forcing mechanism in the Conrad Rise region. However, a mechanism in addition to solar insolation is necessary to explain the delay in deglaciation at the Conrad Rise.

The main source of water at the Conrad Rise is Weddell-sourced Antarctic Bottom Water (Boswell and Smythe-Wright, 2002). The Conrad Rise forms a substantial barrier to the movement of Antarctic Bottom Water and the eastward AAC at all depths. The abundance of biota close to the Conrad Rise may be linked to trapped circulations of these currents that exist over the rise (Durgadoo *et al.*, 2008). On the other hand, the cause of increased sea-ice cover in the Atlantic Sector relative to the Indian Sector is partly dependent on the currents of the Weddell Gyre. Bianchi and Gersonde (2004) inferred that the sea-ice expansion record in the Atlantic Sector is related to the reinforcement and northward expansion of the Weddell Gyre circulation. Current velocities of the Weddell Gyre and the Antarctic bottom water have fluctuated on glacial–interglacial cycles as recorded by the Ti/Al ratios of cores from the northern Weddell Sea (Shimmield *et al.*, 1993). Bottom water velocities increased during the interglacials, including the Holocene. Therefore, we propose that oceanographic shifts in the Weddell Sea directly influenced the water masses at the Conrad Rise, with currents of the Weddell Gyre and the Antarctic Bottom Water shifting eastward at about 10 000 cal a BP. This shift triggered sea-ice retreat in the Atlantic Sector prior to a later change over the Conrad Rise (Fig. 6a).

Following deglaciation, an Early Holocene Optimum (EHO) occurred in the Atlantic Sector and Antarctica from 12 000–11 500 to 9000 cal a BP (Stenni *et al.*, 2001, 2003; Nielsen *et al.*, 2004; Bianchi and Gersonde, 2004), in the central Indian Sector from 12 000 to 9000 cal a BP (Dezileau *et al.*, 2003), in the Pacific Sector from 11 000 to 8500 cal a BP (Denis *et al.*, 2009) and in the Antarctic Peninsula from 11 000 to 9500 cal a BP (e.g. Bentley *et al.*, 2009). Core COR-1PC also clearly records the EHO (Fig. 4). However, the duration of the EHO recorded in the core, as defined by an abrupt peak of the

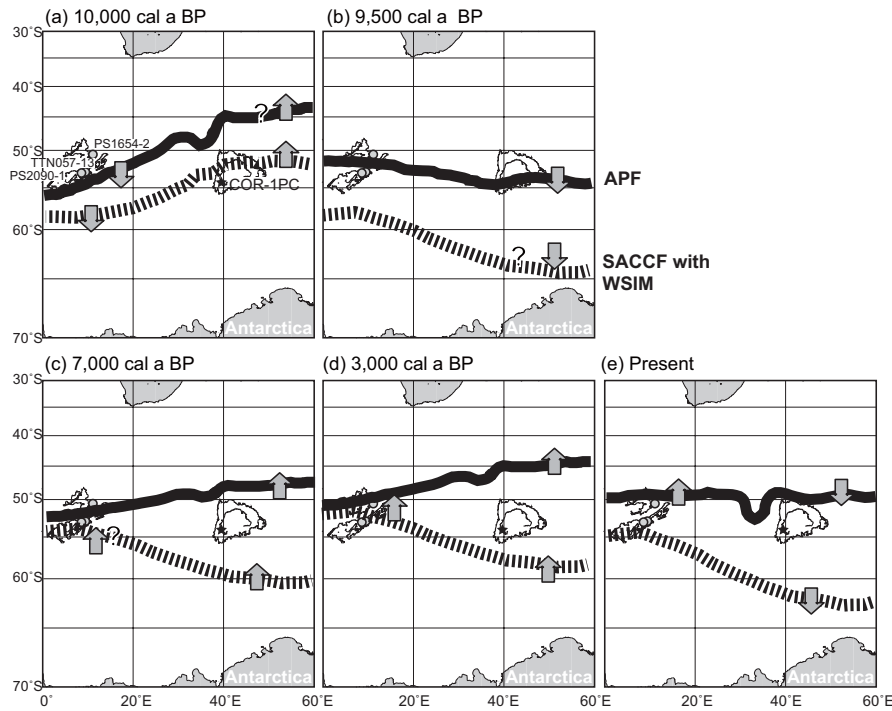


Figure 6. Schematic illustrations depicting the migration of water masses in the Atlantic and Indian sectors: (a) about 10 000 cal a BP, (b) 9500 cal a BP, (c) 7000 cal a BP, (d) 3000 cal a BP and (e) present. Broken lines indicate the boundary of the WSIM, and bold lines indicate the PF. Star, core COR-1PC; shaded circles, cores TTN057-13-PC4 (Hodell *et al.*, 2001) and PS2090 and PS1654 (Bianchi and Gersonde, 2004).

subtropical diatom *Thalassionema nitzschioides* var. *lanceolata* (described by Moreno-Ruiz and Licea, 1996; Romero *et al.*, 2005), is much shorter, from 9900 to 9300 cal a BP, than in the other regions.

Furthermore, *Fragilariopsis kerguelensis*, which indicates open water with no sea-ice cover (e.g. Abelmann *et al.*, 2006), increased in frequency at this time and showed its highest abundance during the Holocene. Indeed, a peak abundance of *F. kerguelensis* is observed around the present-day PFZ, and it is the main component of the Diatom Ooze Belt (Crosta *et al.*, 2005, and references therein). These results indicate that the relatively warm water around the PF moved southward to the Conrad Rise. However, we note that the $\delta^{18}\text{O}$ in core COR-1PC did not decrease during this period.

Differences in diatom taxa and $\delta^{18}\text{O}$ values probably reflect the different living depths of the diatoms and the planktonic foraminifer *Neogloboquadrina pachyderma* (sinistral), the latter being deeper than the former. *N. pachyderma* (sinistral) lives in or just below the chlorophyll maximum zone between 50 and 100 m water depth (Bathmann *et al.*, 1997; Bergami *et al.*, 2009). In the Indian Sector, the temperature of subsurface water (50–200 m depth) under the southern end of the PFZ is similar to that south of the PF, although the surface water south of the PF is warmer (Pollard *et al.*, 2002). Thus, the surface water at the Conrad Rise during the EHO peak was at the southern end of the PF (Fig. 6b). Differences in diatom taxa and $\delta^{18}\text{O}$ values were also confirmed in core PS1654-2 from the Atlantic Sector at 53°S (Bianchi and Gersonde, 2004). The southern end of the PF in the Atlantic Sector reached to 53°S during the EHO peak, similar with the western Indian Sector.

Onset of neoglaciation and changes in insolation

The third stage, from 9300 cal a BP to the present, is characterized by several alternations between cold-water and warm-water conditions (Fig. 4). The cooling spikes in

$\delta^{18}\text{O}$ values appear to correspond to increases in cold-water taxa, although this signal is subtle (Fig. 5). However, low values of sea-ice taxa suggest that sea-ice rarely reached the Conrad Rise throughout the third stage (Fig. 4). Therefore, frontal shifts during the third stage might be limited to a narrow range migration in the Indian Sector. Even at the cooling periods, winter sea-ice maximum (WSIM) did not reach the Conrad Rise.

Based on $\delta^{13}\text{C}$ and $\delta^{18}\text{O}$ values we divide this third stage into three substages: stage 3-1, 9300–4000 cal a BP; stage 3-2, 4000–2500 cal a BP; and stage 3-3, after 2500 cal a BP. During stage 3-1, $\delta^{13}\text{C}$ values continue to increase and $\delta^{18}\text{O}$ values continue to decrease (Fig. 5e, f). Increasing $\delta^{13}\text{C}$ values might be partly explained by increasing sea-surface temperature (SST), which decreases $p\text{CO}_2$ solubility, or by increasing levels of primary productivity. Decreasing $\delta^{18}\text{O}$ values may reflect increasing SST or decreasing salinity. It would appear that these changes indicate that SSTs increased around the Conrad Rise area during stage 3-1. However, the gradual increase of cold-water diatom taxa, particularly *Thalassiosira gracilis* var. *gracilis* (Figs. 5 and 6), indicates the opposite pattern, suggesting that the changes in sub-stage 1 record increasing levels of primary productivity and decreasing salinity and not changes in SST.

Long-term trends in Holocene climate are influenced by a combination of a delayed response to seasonal insolation related to orbital forcing and winter storage of oceanic warmth below the shallow summer mixed layer, particularly in the seasonal sea-ice zone (Renssen *et al.*, 2005). As mentioned previously, the summer solar insolation pattern at 60°S was quite similar to the $\delta^{13}\text{C}$ curve from core COR-1PC (Fig. 5). Therefore, it is probable that the increasing primary productivity was linked to the regional insolation increase. Moreover, it is likely that glacier melting on Antarctica due to the increasing insolation was a cause of salinity and SST decreasing around the Conrad Rise. Glacier retreat from the Antarctic shelf commenced shortly after the Last Glacial Maximum and continued into the late Holocene in

West Antarctica. In particular, the glaciers of many presently ice-free areas retreated in the early Holocene (Ingólfsson *et al.*, 1998; Anderson *et al.*, 2002). However, *F. kerguelensis*, which occurs today within the PFZ, decreased gradually during this period (Fig. 4) suggesting that the PFZ moved northward away from the Conrad Rise during stage 3-1.

During stage 3-1, the Conrad Rise was located to the north of the WSIM, and to the south of the APF, as indicated by diatom taxa (Fig. 6c). On the other hand, diatom assemblages were also analysed from sediment cores at the same latitude (about 53°11'S, 5°8'E), in the eastern Atlantic Sector: core TTN057-1 (Hodell *et al.*, 2001) and core PS2090-1 (Bianchi and Gersonde, 2004). At present, these cores are also located between the WSIM and the APF (Fig. 6). Sedimentation rates of these cores were quite high, between 14 and 125 cm ka⁻¹, higher than that of core COR-1PC. Even though the sites of cores TTN057-13 and PS2090-1 are very close together, diatom assemblages in core TTN057-1 lay to the north of the APF during stage 3-1, based on the summer SST (4–5°C); however, the diatom assemblage in core PS2090-1 conversely indicates that the PF was located to the north of this site, based on summer SST (0–1°C) values, and the WSIM extended to this. Thus, we infer that the PF and WSIM were adjacent at about 53°S in the Atlantic Sector during stage 3-1 (Fig. 6c).

During stage 3-2 (4000–2500 cal a BP), $\delta^{18}\text{O}$ values decreased, although $\delta^{13}\text{C}$ values continued to increase and reached a maximum at 2500 cal a BP. The percentage of *T. gracilis* var. *gracilis* also gradually increased until 3000 cal a BP, when it reached a maximum (Fig. 4). We interpret the start of a decline in $\delta^{18}\text{O}$ values at about 4000 cal a BP as evidence for the onset of neoglaciation at the Conrad Rise. Elsewhere in the Southern Ocean this event is reported at around 5000 cal a BP in the high-latitude Atlantic Sector (Hodell *et al.*, 2001), at around 3300–3700 cal a BP on the western Antarctic Peninsula (e.g. Taylor *et al.*, 2001; Domack *et al.*, 2003), and at around 3900 cal a BP along the eastern Antarctic coast (Crosta *et al.*, 2007, 2008). Low SST values between 4000 and 2500 cal a BP, despite high solar insolation, were probably associated with the onset of Antarctic coastal neoglaciation where spring SST was 1–2°C lower compared with the mid-Holocene (e.g. Crosta *et al.*, 2008). Furthermore, the duration of sea-ice cover lengthened during this neoglaciation based on changes in diatom assemblage and sediment structure in the coastal region of Antarctica (e.g. Taylor *et al.*, 2001; Crosta *et al.*, 2007, 2008). High primary productivity at the Conrad Rise, indicated by the high $\delta^{13}\text{C}$ values during this period, was probably related to high levels of insolation and melt-water input (Fig. 6d). Increased light in early spring, combined with melt-water stratification of the upper water column, supports large algal blooms (e.g. Abbott *et al.*, 2000). The decline in frequencies of *F. kerguelensis* during this period (Fig. 4) probably indicates that the PFZ moved further northward away from the Conrad Rise (Fig. 6d).

During stage 3-2, SST at about 53°S in both the Atlantic and Indian sectors is inferred to have decreased. The WSIM extended northward of 53°S in the Atlantic Sector (Hodell *et al.*, 2001; Bianchi and Gersonde, 2004) but not in the Indian Sector, as mentioned above. The diatom assemblages of core PS1654-2 (Bianchi and Gersonde, 2004) suggest that the site, at about 50°S, was not covered by winter sea-ice, and summer SST was 3–4°C. At that time, the PF and WSIM were situated between 50 and 53°S in the Atlantic Sector (Fig. 6d).

After 2500 cal a BP, during stage 3-3, primary productivity as reflected in $\delta^{13}\text{C}$ values decreased on the Conrad Rise (Fig. 5). According to the $\delta^{18}\text{O}$ values in Core COR-1PC, SSTs in this region increased again around 2000 cal a BP (Hodell *et al.*, 2001) and the WSIM retreated in the Atlantic Sector during this

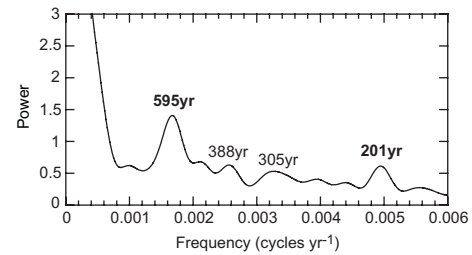


Figure 7. Oxygen isotope spectral analysis for core COR-1PC. The bandwidth for the Blackman–Tukey method was 0.0005. Spectral analysis was performed using the program AnalySeries 2.0 (Paillard *et al.*, 1996).

period. In comparison with the present oceanographic condition, the WSIM retreated after this date, particularly in the Indian Sector (Fig. 6e).

High-frequency variability in solar irradiance

Multicentennial-scale variability in SSTs is recorded throughout the third stage in core COR-1PC (Fig. 5; Table 1). Spikes in $\delta^{18}\text{O}$ values in core COR-1PC recur approximately every 200 a based on spectral analysis (Fig. 7). The isotopic spikes coincide with the timing of increases in cold-water diatom species in core COR-1PC (Fig. 5), indicating that a small SST change about every 200 a had a considerable influence on primary productivity. This 200-a periodicity in the Holocene has been reported from many places in the Southern Hemisphere: for example, fluctuations in tree-ring ^{14}C data (Stuiver and Braziunas, 1993; Cook *et al.*, 1996), magnetic susceptibility and organic carbon in continental shelf sediments (Leventer *et al.*, 1996).

This periodicity may be explained by fluctuations in solar activity amplified by atmospheric (Crosta *et al.*, 2007) and internal oscillations of the climate system, such as albedo and oceanic thermohaline feedback (Stuiver and Braziunas, 1993; Leventer *et al.*, 1996; Masson *et al.*, 2000). Amplifications in solar activity result in greater absorption of UV radiation by stratospheric ozone, raising temperatures and producing stronger winds in the lower troposphere (Shindell *et al.*, 1999). This leads to relocation of storm tracks and pressure cells. Along the coast of Antarctica, off Adélie Land, strong variations in storms affected the area covered by sea-ice as well as the dominant diatom taxa during the Holocene (Denis *et al.*, 2006; Crosta *et al.*, 2007). Similarly, it seems that pressure pattern changes were related to solar activity control of SST and sea-surface biota at the Conrad Rise. The extent of sea-ice in coastal regions affects SST in the neighbouring ocean. This relationship is supported by δD spikes of the east Antarctic ice core, particularly in the Vostok core (Petit *et al.*, 1999), and atmospheric $\Delta^{14}\text{C}$ values (Stuiver *et al.*, 1991) that coincide with the timing of increases in the abundance of cold-water diatoms in core COR-1PC (Fig. 5).

Conclusions

Detailed information on Holocene palaeoenvironmental changes is provided by the diatom assemblages and stable isotope data of core COR-1PC from the Conrad Rise in the western Indian Sector of the Southern Ocean. Holocene oceanographic changes at the Conrad Rise were associated with long-term shifts in water masses, changes in insolation and short-term solar activity. The following conclusions are based on the reconstruction of the shifts in regional oceanographic fronts:

- (1) Sea-ice cover at the Conrad Rise retreated at 9900 cal a BP. The timing of this retreat was about 1500 a later than shifts in Antarctic climate and sea-ice retreat in other sectors.
- (2) A short early Holocene optimum is preserved in core COR-1PC after the sea-ice retreat. At that time, the APF is thought to have been over this location influencing the surface waters above the Conrad Rise.
- (3) Neoglaciation began at around 4000 a BP. Its onset was delayed compared with that in the Atlantic Sector. The range of oceanographic front migration was narrow at that time.
- (4) Between 4000 and 2500 cal a BP, SST decreased on the Conrad Rise at the same time as Antarctic coastal region cooling. The WSIM reached to 53°S in the Atlantic Sector, but did not extend this far north in the Indian Sector. Primary productivity at the Conrad Rise reached a maximum during this period.
- (5) Atmospheric pressure pattern changes resulting from changes in solar activity drove SST and sea-surface biota oscillations with a 200-a periodicity; however, the fluctuations were minor.

Acknowledgements. We are grateful to chief scientist Dr Y. Nogi (National Institute of Polar Research), and the captain, crew, scientists and students of Cruise KH07-04 onboard R/V *Hakuho-Maru* in 2008. We also appreciate the analytical assistance provided by M. Kobayashi. Financial support from MEXT Grants-in-Aid-for Scientific Research (B), Project No. 19340156 (to M. Ikehara) and the KOPRI project (PP11010 to B.K. Khim) is gratefully acknowledged. Y. Yokoyama's work was partly supported by Grants-in-Aid for Scientific Research Project Nos. 21674003, 19340158 and 20300294; NEXT program (GR031); GCOE; and Global Environmental Research Fund RF-081.

Abbreviations. AAZ, Antarctic Zone; ACC, Antarctic Circumpolar Current; AMS, accelerator mass spectrometry; APF, Antarctic Polar Front; EHO, Early Holocene Optimum; PFZ, Polar Frontal Zone; SACCF, Southern ACC Front; SAF, Subantarctic Front; SST, sea-surface temperature; STF, Subtropical Front; WSIM, winter sea-ice maximum.

References

- Abbott MR, Richman JG, Letelier RM, *et al.* 2000. The spring bloom in the Antarctic Polar Frontal Zone as observed from a mesoscale array of bio-optical sensors. *Deep-Sea Research II* **47**: 3285–3314.
- Abelmann A, Gersonde R, Cortese G, *et al.* 2006. Extensive phytoplankton blooms in the Atlantic sector of the glacial Southern Ocean. *Paleoceanography* **21**: PA1013. DOI: 10.1029/2005PA001199.
- Anderson JB, Shipp SS, Lowe AL, *et al.* 2002. The Antarctic Ice Sheet during the Last Glacial Maximum and its subsequent retreat history: a review. *Quaternary Science Reviews* **21**: 49–70.
- Armand LK, Crosta X, Romero O, *et al.* 2005. The biogeography of major diatom taxa in Southern Ocean sediments: 1. Sea ice related species. *Palaeogeography, Palaeoclimatology, Palaeoecology* **223**: 93–126.
- Bard E. 1988. Correction of accelerator mass spectrometry ¹⁴C ages measured in planktonic foraminifera: paleoceanographic implications. *Paleoceanography* **3**: 635–645.
- Bareille G, Labracherie M, Labeyrie L, *et al.* 1991. Biogenic silica accumulation rate during the Holocene in the Southeastern Indian Ocean. *Marine Chemistry* **35**: 537–551.
- Bathmann UV, Scharek R, Klaas C, *et al.* 1997. Spring development of phytoplankton biomass and composition in major water masses of the Atlantic sector of the Southern Ocean. *Deep-Sea Research II* **44**: 51–67.
- Belkin IM, Gordon AL. 1996. Southern Ocean fronts from the Greenwich Meridian to Tasmania. *Journal of Geophysical Research* **101**: 3675–3696.
- Bentley MJ, Hodgson DA, Smith JA, *et al.* 2009. Mechanisms of Holocene palaeoenvironmental change in the Antarctic Peninsula region. *Holocene* **19**: 51–69.
- Bergami C, Capotondia L, Langonea L, *et al.* 2009. Distribution of living planktonic foraminifera in the Ross Sea and the Pacific sector of the Southern Ocean (Antarctica). *Marine Micropaleontology* **73**: 37–48.
- Berger AL. 1978. Long-term variation of daily insolation and Quaternary climate change. *Journal of the Atmospheric Sciences* **35**: 2362–2367.
- Bianchi C, Gersonde R. 2004. Climate evolution at the last deglaciation: the role of the Southern Ocean. *Earth and Planetary Science Letters* **228**: 407–424.
- Boswell SM, Smythe-Wright D. 2002. The tracer signature of Antarctic Bottom Water and its spread in the Southwest Indian Ocean: part IFCFC-derived translation rate and topographic control around the Southwest Indian Ridge and the Conrad Rise. *Deep-Sea Research I* **49**: 555–573.
- Cook E, Buckley BM, D'Arrigo RD. 1996. Inter-decadal climate oscillations in the Tasmanian sector of the Southern Hemisphere: evidence from tree rings over the past three millennia. In *Forcing Mechanisms of the Last 2000 years*, NATO ASI Ser, Ser I, 141, Jones PD, Bradley RS, Jouzel J (eds). Springer: New York; pp. 141–160.
- Crosta X, Romero O, Armand LK, *et al.* 2005. The biogeography of major diatom taxa in Southern Ocean sediments: 2. Open ocean related species. *Palaeogeography, Palaeoclimatology, Palaeoecology* **223**: 66–92.
- Crosta X, Debret M, Denis D, *et al.* 2007. Holocene long- and short-term climate changes off Adélie Land, East Antarctica. *Geochemistry, Geophysics, Geosystems* **8**: Q11009. DOI: 10.1029/2007GC001718.
- Crosta X, Denis D, Ther O. 2008. Sea ice seasonality during the Holocene, Adélie Land, East Antarctica. *Marine Micropaleontology* **66**: 222–232.
- de Baar HJW, de Jong JTM, Bakker DCE, *et al.* 1995. Importance of iron for plankton blooms and carbon dioxide drawdown in the Southern Ocean. *Nature* **373**: 412–415.
- Denis D, Crosta X, Zaragosi S, *et al.* 2006. Seasonal and sub-seasonal climate changes recorded in laminated diatom ooze sediments, Adélie Land, East Antarctica. *Holocene* **16**: 1137–1147.
- Denis D, Crosta X, Schmidt S, *et al.* 2009. Holocene glacier and deep water dynamics, Adélie Land region, East Antarctica. *Quaternary Science Reviews* **28**: 1291–1303.
- Dezileau L, Reyss JL, Lemoine F. 2003. Late Quaternary changes in biogenic opal fluxes in the Southern Indian Ocean. *Marine Geology* **202**: 143–158.
- Domack EW, Leventer A, Root S, *et al.* 2003. Marine sedimentary record of natural environment variability and recent warming in the Antarctic Peninsula. In *Antarctic Peninsula Climate Variability*, Domack EW, Leventer A, Burnett A, Bindschadler R, Convey P, Kirby M (eds). American Geophysical Union: Washington, DC; pp. 205–224.
- Durgadoo JV, Lutjeharms JRE, Biastoch A, *et al.* 2008. The Conrad Rise as an obstruction to the Antarctic Circumpolar Current. *Geophysical Research Letters* **35**: L20606. DOI: 10.1029/2008GL035382
- Gersonde R, Zielinski U. 2000. The reconstruction of late Quaternary Antarctic sea-ice distribution – The use of diatoms as a proxy for sea-ice. *Palaeogeography, Palaeoclimatology, Palaeoecology* **162**: 263–286.
- Gersonde R, Abelmann A, Brathauer U, *et al.* 2003. Last glacial sea surface temperatures and sea-ice extent in the Southern Ocean (Atlantic-Indian sector): a multiproxy approach. *Paleoceanography* **18**: 1061. DOI: 10.1029/2002PA 000809.
- Hodell DA, Kanfoush SL, Shemesh A, *et al.* 2001. Abrupt cooling of Antarctic surface waters and sea ice expansion in the South Atlantic Sector of the Southern Ocean at 5000 cal yr B.P. *Quaternary Research* **56**: 191–198.
- Ingólfsson Ó, Hjort C, Berkman PA, *et al.* 1998. Antarctic glacial history since the Last Glacial Maximum: an overview of the record on land. *Antarctic Science* **10**: 326–344.
- Jouzel J, Masson V, Cattani O, *et al.* 2001. A new 27 ky high resolution East Antarctic climate record. *Geophysical Research Letters* **28**: 3199–3202.

- Leventer A, Domack EW, McClennen CE, *et al.* 1996. Productivity cycles of 200–300 years in the Antarctic Peninsula region: understanding linkages among the sun, atmosphere, oceans, sea ice, and biota. *Geological Society of America Bulletin* **108**: 1626–1644.
- Lisitzin AP. 1972. Sedimentation in the world Ocean. *Society of Economic Paleontology and Mineral Special Publication* 17.
- Lorius C, Merlivat L, Jouzel J, *et al.* 1979. A 30,000 yr isotope climatic record from Antarctic ice. *Nature* **280**: 644–648.
- Masson V, Vimeux F, Jouzel J, *et al.* 2000. Holocene climate variability in Antarctica based on 11 ice-core isotopic records. *Quaternary Research* **54**: 348–358. DOI: 10.1006/qres.2000.2172.
- Moreno-Ruiz JL, Licea S. 1996. Observations on the valve morphology of *Thalassionema nitzschioides* (Grunow) Hustedt. In *Proceedings of 13th International Diatom Symposium*, Marino D, Montresor M (eds). Biopress Ltd, Bristol; pp. 393–413.
- Morgan V, Delmotte M, van Ommen T, *et al.* 2002. Relative timing of deglacial climate events in Antarctica and Greenland. *Science* **297**: 1862–1864.
- Nielsen SHH, Koc N, Crosta X. 2004. Holocene climate in the Atlantic sector of the Southern Ocean: controlled by insolation or oceanic circulation? *Geology* **32**: 317–320. DOI: 10.1130/G20334.1.
- Orsi AH, Whitworth T, Nowlin WD. 1995. On the meridional extent and fronts of the Antarctic Circumpolar Current. *Deep-Sea Research I* **42**: 641–673.
- Paillard D, Labeyrie L, Yiou P. 1996. Macintosh program performs time-series analysis. *EOS Transactions AGU* **77**: 379.
- Paillard D. 1998. The timing of Pleistocene glaciations from a simple multiple-state climate model. *Nature* **391**: 378–381.
- Petit JR, Jouzel J, Raynaud D, *et al.* 1999. Climate and atmospheric history of the past 420,000 years from the Vostok Ice Core, Antarctica. *Nature* **399**: 429–436.
- Pollard RT, Lucas MI, Read JF. 2002. Physical controls on biogeochemical zonation in the Southern Ocean. *Deep-Sea Research II* **49**: 3289–3305.
- Renssen H, Goosse H, Fichefet T, *et al.* 2005. Holocene climate evolution in the high-latitude Southern Hemisphere simulated by a coupled atmosphere-sea-ice-ocean-vegetation model. *Holocene* **15**: 951–964.
- Romero OE, Armand TLK, Crosta X, *et al.* 2005. The biogeography of major diatom taxa in Southern Ocean surface sediments: 3. Tropical/Subtropical species. *Palaeogeography, Palaeoclimatology, Palaeoecology* **223**: 49–65.
- Shimmield G, Derrick S, Pudsey C, *et al.* 1993. The use of inorganic chemistry in studying the paleoceanography of the Weddell Sea. In *University Research in Antarctica: Proceedings of British Antarctic Survey Antarctic Special Topic Award Scheme Symposium*, 9–10 November 1988. Heywood RB (ed). British Antarctic Survey: Cambridge; pp. 99–108.
- Shindell D, Rind D, Balachandran N, *et al.* 1999. Solar cycle variability, ozone, and climate. *Nature* **284**: 305–308.
- Simmonds I, Jacka TH. 1995. Relationships between the interannual variability of Antarctic sea-ice and the Southern Oscillation. *Journal of Climate* **8**: 637–647.
- Sparrow MD, Heywood KJ, Brown J, *et al.* 1996. Current structure of the south Indian Ocean. *Journal of Geophysical Research* **101**: 6377–6391.
- Stenni B, Masson-Delmotte V, Johnsen S, *et al.* 2001. An oceanic cold reversal during the last deglaciation. *Science* **293**: 2074–2077.
- Stenni B, Jouzel J, Masson-Delmotte V, *et al.* 2003. A late-glacial high-resolution site and source temperature record derived from the EPICA Dome C isotope records (East Antarctica). *Earth and Planetary Science Letters* **217**: 183–195.
- Stuiver M, Braziunas TF, Becker B, *et al.* 1991. Climatic, solar, oceanic, and geomagnetic influences on late-glacial and Holocene atmospheric $^{14}\text{C}/^{12}\text{C}$ change. *Quaternary Research* **35**: 1–24.
- Stuiver M, Braziunas TF. 1993. Sun, ocean, climate and atmospheric $^{14}\text{CO}_2$: an evaluation of causal and spectral relationships. *Holocene* **3**: 289–305.
- Stuiver M, Reimer PJ, Bard E, *et al.* 1998. INTCAL98 radiocarbon age calibration, 24,000–0 cal BP. *Radiocarbon* **40**: 1041–1083.
- Taylor F, Whitehead J, Domack E. 2001. Holocene paleoclimate change in the Antarctic Peninsula: evidence from the diatom, sedimentary and geochemical record. *Marine Micropaleontology* **41**: 25–43.
- Yokoyama Y, Miyairi Y, Matsuzaki H, *et al.* 2007. Relation between acid dissolution time in the vacuum test tube and time required for graphitization for AMS target preparation. *Nuclear Instruments and Methods in Physics Research Section B* **259**: 330–334.
- Yokoyama Y, Koizumi M, Matsuzaki H, *et al.* 2010. Developing ultra small scale radiocarbon sample measurement at the University of Tokyo. *Radiocarbon* **52**: 310–318.
- Zielinski U, Gersonde R. 1997. Diatom distribution in Southern Ocean surface sediments (Atlantic sector): Implications for paleoenvironmental reconstructions. *Palaeogeography, Palaeoclimatology, Palaeoecology* **129**: 213–250.